A Vibrational Spectroscopic Investigation of Interactions of Agonists with GluR0 a Prokaryotic Glutamate Receptor†

Qing Cheng,§ Shalita Thiran,§ Dinesh Yernool,# Eric Gouaux,#,‡ and Vasanthi Jayaraman*,§

Chemistry Department, Marquette University, Milwaukee, Wisconsin 53233, and Howard Hughes Medical Institute and Department of Biochemistry and Molecular Biophysics, Columbia University, 650 West 168th Street, New York, New York 10032

Received August 29, 2001; Revised Manuscript Received December 10, 2001

ABSTRACT: We have used Fourier transform infrared spectroscopy to provide a detailed picture of the interactions between the carboxylate groups of the ligands, glutamate, serine, and glutamine, with the ligand-binding domain of a prokaryotic ionotropic glutamate receptor (GluR0). The vibrational spectra indicate that the noncovalent interactions between the 1C(α)-carboxylate moiety of the ligand and the protein are stronger for glutamate than for serine and glutamine. These results correlate well with the higher affinity of glutamate for GluR0−S1S2 relative to the affinities of serine and glutamine. In addition, all three ligands induce similar changes in the vibrational spectra and intrinsic fluorescence of the protein, which indicates that all three ligands induce the same structural changes in the protein. These results are consistent with the recent crystal structures of the glutamate and serine bound forms of GluR0−S1S2 and in addition provide insights into the structure of the glutamine bound form of the protein.

Ionotropic glutamate receptors are transmembrane proteins, which mediate fast excitatory responses in the central nervous system through the formation of ligand-gated ion channels (*1*−*4*). On the basis of their agonist binding profiles, these receptors have been conventionally classified into α-amino-5-methyl-3-hydroxy-4-isoxazole propionate (AMPA),[1] *N*-methyl-D-aspartate, and kainate receptors (*5*, *6*). More recently, a prokaryotic ionotropic glutamate receptor (GluR0) has been discovered that exhibits significant sequence homology with the eukaryotic glutamate receptor subunits (*7*). Contrary to the eukaryotic receptor, the GluR0 is not gated by classical glutamate receptor agonists such as AMPA, kainate, or NMDA. However, GluR0 is activated by a large number of L-α-amino acids such as glutamate, serine, and glutamine (*7*). Furthermore, electrophysiological measurements indicate that the GluR0 receptors form transmembrane ion channels that are selectively permeable to K^+ ions, while the eukaryotic receptors form channels that are permeable to both Na^+ and K^+ ions. Single channel measurements of the GluR0 indicate a large number of spontaneous openings in the unligated form (personal communication Mayer, M. L.). However, the kinetics of activation, as measured by the 10−90% rise time for the whole cell currents, are much slower (290 ± 15 ms) for the GluR0 than the corresponding rise time for the GluR2 homomeric receptors (18 ± 3 ms) (*7*). These differences in the agonist binding profiles and, to some extent, the differences in the electrophysiological properties between the GluR0 and GluR2 receptor can be related to differences at the ligand binding domains of the two receptors. The large scale expression of the soluble ligand binding domains (S1S2) of the GluR0 and GluR2, and the subsequent characterization of the crystal structures of these protein in the apo and ligated forms has provided significant insights into some of these differences in the ligand protein interactions and structural changes at the ligand binding site.

The structures of GluR2−S1S2 protein in the apo form and in complex with agonists and antagonists (*8*) indicate that the ligand-binding domain is a bilobate structure and the degree of cleft closure between the two lobes is related to the type of ligand bound to the protein. Full agonists such as glutamate and AMPA induce a 20° closure of the two domains relative to the apo form, while the partial agonist kainate induces only a 12° closure of the two domains. On the other hand, the antagonist DNQX bound form does not exhibit any large conformational changes relative to the apo form (*8*). These results suggest that the degree of domain closure most likely controls the extent of channel activation, thus providing the first structural insight into the activation mechanism of the glutamate receptors. The more recent structures of the GluR0−S1S2 in the apo, glutamate, and serine bound forms indicate that the protein adopts a similar bilobate structure as the GluR2−S1S2 protein (*9*). These structures exhibit no significant changes in the degree of domain closure between the apo and ligated forms. Further,

† This work was supported by the National Science Foundation Grants NSF-9982759 and NSF-0096635 (V.J.), and National Institute of Health (E.G.). E.G. is an assistant investigator of the Howard Hughes Medical Institute.

* To whom correspondence should be addressed: Vasanthi Jayaraman, Chemistry Department, Marquette University, Milwaukee, WI 53233. Telephone: 414-288-7859. Fax: 414-288-7066. E-mail: vasanthi.jayaraman@marquette.edu.

§ Marquette University.

‡ Howard Hughes Medical Institute, Columbia University.

Department of Biochemistry and Molecular Biophysics, Columbia University.

[1] Abbreviations: α-Amino-5-methyl-3-hydroxy-4-isoxazole propionate (AMPA), *N*-methyl-D-aspartate (NMDA), glutamate receptor (GluR), Fourier transform infrared spectroscopy (FTIR).

10.1021/bi015729e CCC: $22.00
Published on Web 01/10/2002

the structures of glutamate and serine bound forms of GluR0−S1S2 are similar, with comparable degrees of cleft closure.

A more detailed investigation of specific interactions between the ligands kainate and glutamate with the eukaryotic GluR4−S1S2 has also been obtained using vibrational spectroscopy (*10*). The inherent sensitivity of the vibrations of the carboxylate moieties of the ligand to its electronic environment permitted a detailed investigation of the interactions between these moieties of the ligands with the protein. Further, the amide I vibrations of the protein backbone, which is sensitive to the secondary structure of the protein, indicated larger changes in the protein upon binding glutamate relative to kainate. The results from these spectroscopic investigations were consistent with crystallographic data, and extended the structural information by providing a more detailed picture of the strength of the important interactions between the ligand and protein.

In the present report, we have performed a similar vibrational spectroscopic study to investigate the interactions between the ligands glutamate, serine, and glutamine with the GluR0−S1S2 protein. The vibrational spectra reveal differences in the interactions of the three ligands with the protein that qualitatively correlate to the differences in the affinity of these ligands with the GluR0−S1S2. In addition, the FTIR and fluorescence measurements indicate that the three ligands induce similar changes in the GluR0−S1S2. These results suggest that the recent crystal structures of GluR0−S1S2 in complex with glutamate, and serine could be extended to describe the structure of GluR0−S1S2 in complex with glutamine.

MATERIALS AND METHODS

Protein Preparation. The GluR0−S1S2 protein used in the present experiments was the same as that used by Mayer et al. (*9*). The GluR0−S1S2 construct contains the S1 segment comprising of amino acids 43 to 139 in the GluR0 sequence (*7*, *9*) and the S2 segment consisting of amino acids 256 to 385 in the GluR0 sequence, with the two domains linked by a two amino acid (GT) linker.

The protein was expressed, purified, and characterized as described in refs *7* and *9*. In brief, the His tag labeled S1S2 construct (*7*, *9*) of GluR0 was expressed in *Escherichia coli* cells. The *E. coli* cells obtained by centrifugation were disrupted, and the lysate was clarified by centrifugation. The GluR0−S1S2 was then isolated from the supernantant using a Ni NTA column. The His tag of the GluR0−S1S2 eluent from the nickel column was cleaved using thrombin, and the protein was purified using an anion exchange column. The purified protein was concentrated and dialyzed to yield a final concentration of ~0.5 to 1 mM in 25 mM phosphate buffer containing 250 mM NaCl and 0.02% NaN_3, pD 7.4.

FTIR Difference Spectroscopy. The FTIR spectra were measured on a Nicolet Magna 870 infrared spectrophotometer, using an FTIR cell with CaF_2 windows and a 75-micron spacer. Spectra were collected at 4 cm^{-1} spectral resolution. The sample holder (Aldrich, Milwaukee, WI) was modified to allow liquid from a constant-temperature bath to circulate around the holder, ensuring that the protein solutions were kept at a constant temperature of 15 °C.

The spectra were recorded in blocks of 500 scans, and four such spectra were added to obtain the final spectrum.

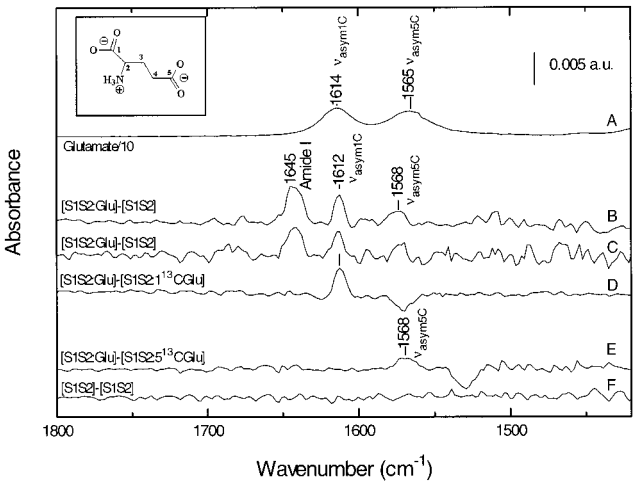

FIGURE 1: Difference FTIR spectrum between (A) glutamate and D_2O, (B) glutamate-bound and unligated form of GluR0 S1S2 protein in D_2O obtained at saturating concentrations of glutamate, (C) glutamate-bound and unligated form of GluR0 S1S2 protein in D_2O obtained at a 10-fold lower concentration of glutamate relative to protein, (D) glutamate-bound and 1C-^{13}C glutamate-bound form of GluR0 S1S2 protein in D_2O, and (E) glutamate-bound and 5C-^{13}C glutamate-bound form of GluR0 S1S2 protein in D_2O. (F) Two consecutive 500 scans of protein. The structure of glutamate is shown in the inset.

Before adding the blocks, the spectra were subtracted from one another to ensure that no differences were observed between the spectra.

All spectra reported are difference spectra, and the subtraction was performed using the band at 2045 cm^{-1} arising from the sodium azide present in the buffer as an internal standard. Furthermore, for generating the difference spectra between the ligand bound and apo forms of the protein, the peaks that arise from excess unbound ligand (glutamate, serine, and glutamine) were subtracted using the spectrum of the ligand. Control experiments were also performed using 1 mM protein in the absence and presence of 100 μM ligand, and the difference spectrum was generated using the azide band as the internal standard; under these conditions since K_d values for glutamate, glutamine, and serine are 0.21 ± 0.02, 0.8 ± 0.1, 1.7 ± 0.7 μM the ligands exists predominantly in the bound form. Although these spectra exhibited a lower signal-to-noise ratio (Figure 1, trace C), they provided an additional basis for determining the appropriate scaling factor in the generation of difference spectra at saturating concentrations of ligand. Because water (H_2O) has a large infrared absorption band at ~1600 cm^{-1}, D_2O was used as the solvent to obtain spectra in the 1450−1800 cm^{-1} region. The frequencies for the peaks in the spectra were determined by curve-fitting the peaks using a mixture of Gaussian and Lorentzian functions.

Model Compound Studies. To determine the $\nu_{a,COOH}$ frequency, 10 mM tetrabutylammonium acetate was dissolved in DMSO and the FTIR spectrum obtained in the 1000 to 2000 cm^{-1} region in the presence of guanidine derivatives. A 1:1 concentration ratio of acetate to guanidine was used to determine the $\nu_{a,COOH}$ frequency of acetate in association with 1,1-dimethylguanidine tetraphenylborate. To investigate the $\nu_{a,COOH}$ frequency of acetate in association with guanidine tetraphenylborate, a 1:1 concentration ratio of acetate to guanidine was used to determine the effect due to first binding step, and a 2:1 concentration ratio of acetate to

guanidine was used to determine the effect due to second binding step. The $\nu_{a,COOH}$ vibrational mode in the spectrum of the 2:1 concentration ratio of acetate to guanidine tetraphenylborate was curve fitted to two peaks, while the $\nu_{a,COOH}$ vibrational mode in the 1:1 ratio of acetate to guanidine derivatives were fit with one peak using a mixture of Gaussian and Lorentzian functions.

Fluorescence Spectroscopy. The fluorescence spectra were measured using a Jasco FP-6500 spectrofluorometer and at least three measurements were performed at each ligand concentration. The excitation wavelength was 280 nm and the emission intensity was measured at 335 nm for the fluorescence titration measurements. The excitation band-pass was 4 nm, and the emission band-pass was 8 nm. For the titration measurements, 3 μL of concentrated ligand solution was added to 3 mL of 10 nM protein solution in phosphate buffer (pH 7.4). The fluorescence change observed at 335 nm was corrected for dilution of the protein sample with the ligand. The fluorescence measurements were performed at 4 °C.

The fluorescence titration curves were fit using eq 1, which represents the fluorescence change in the protein for a single step ligand-binding mechanism.

$$\Delta F = \Delta F_{max} \otimes \left[\frac{(P_0 + L_0 + K_d) - \sqrt{(P_0 + L_0 + K_d)^2 - (4 \otimes P_0 \otimes L_0)}}{2 \otimes P_0}\right] \quad (1)$$

Where ΔF is the change in the fluorescence signal, ΔF_{max} is the maximum change in fluorescence signal, P_0 is the initial protein concentration, L_0 is the initial ligand concentration, and K_d is the dissociation constant of the ligand.

RESULTS

Ligand Environment. The frequency associated with the asymmetric carboxylate stretching vibration ($\nu_{a,COOH}$) is extremely sensitive to the overall electrostatic and hydrogen bonding environment of the carboxylate moiety (*11*−*13*). Thus, monitoring the changes in $\nu_{a,COOH}$ has proven a facile mechanism to investigate the chemical environments of ligands with carboxylate groups as demonstrated by Jayaraman et al. in a previous study of GluR4−S1S2 (*10*). In this report, we have performed a similar investigation of the interactions of glutamate, serine, and glutamine with the ligand-binding domain of the prokaryotic glutamate receptor (GluR0−S1S2) using infrared spectroscopy to monitor the asymmetric carboxylate vibrations of the above ligands.

The vibrational spectrum of glutamate in D_2O, in the region 1750 cm^{-1} to 1350 cm^{-1}, is shown in Figure 1 (trace A). On the basis of normal mode calculations (*13*) and isotopic labeling studies (*10*), the absorption band at 1614 cm^{-1}, in the spectrum of glutamate in D_2O, is assigned to the asymmetric vibrational stretching mode of the 1C carboxylate group (ν_{asym1C}), and the absorption band at 1565 cm^{-1} is assigned to the asymmetric vibrational stretching vibration of the 5C carboxylate group (ν_{asym5C}).

To examine the changes in the ν_{asym1C} and ν_{asym5C} modes of the glutamate bound to the GluR0−S1S2 protein, a difference spectrum between the glutamate-bound and unligated forms of the protein was obtained and is shown as trace B in Figure 1. In addition to the features corresponding to the bound glutamate, this difference spectrum also contains band(s) arising from changes in the protein induced by glutamate binding. To identify and distinguish the bands due to the bound glutamate from those due to changes in the protein because of the glutamate binding, difference spectra were obtained using glutamate isotopically labeled with ^{13}C at the 1C (α) and 5 C (γ) positions.

Table 1: Vibrational Modes of the Ligands and GluR0−S1S2

	ν_{asym1C} (cm^{-1})		ν_{asym5C} (cm^{-1})		amide I (cm^{-1})
ligand	free	bound to S1S2	free	bound to S1S2	protein
glutamate	1614	1612	1565	1568	1645
serine	1619	1619			1645
glutamine	1619	1619			1645

The difference spectrum between the protein bound to unlabeled glutamate and the protein bound to 1C-^{13}C glutamate is shown in trace D of Figure 1. This spectrum exhibits a positive band at 1612 cm^{-1} and a negative band at 1570 cm^{-1} (see Table 1 for frequencies and assignments). The positive peak at 1612 cm^{-1} reflects the unlabeled ν_{asym1C} mode of the bound glutamate, while the negative peak at 1570 cm^{-1} is the ν_{asym1C} mode downshifted because of isotopic labeling at the 1C position. Similarly, the difference spectrum between the protein bound to unlabeled glutamate and the protein bound to 5C-^{13}C glutamate, shown in trace E of Figure 1, exhibits a positive band at 1568 cm^{-1} and a negative band at 1529 cm^{-1}. The positive and negative peaks correspond to the unlabeled and labeled asymmetric vibrations of the 5C carboxylates of glutamate, respectively. Comparing these values for the frequencies of the ν_{asym1C} and ν_{asym5C} of the bound glutamate with the frequencies of the glutamate in D_2O (Table 1), it is observed that the ν_{asym1C} mode is downshifted by 2 cm^{-1} ($\Delta_{\nu asym1C} = -2$ cm^{-1}) while the ν_{asym5C} mode is upshifted by 3 cm^{-1} ($\Delta_{\nu asym5C} = +3$ cm^{-1}) in the protein relative to D_2O.

Model Compounds Studies. To correlate these shifts in the vibrational modes to changes in the environment of glutamate, we have examined the $\nu_{a,COOH}$ for tetrabutylammonium acetate in complex with two guanidine derivatives exhibiting different enthalpies for the association (Figure 2). The two guanidine derivatives used are 1,1-dimethylguanidine tetraphenylborate that forms a 1:1 complex with tetrabutylammonium acetate ($\Delta H = -3.8 \pm 0.1$) and guanidine tetraphenylborate that associates with two acetate molecules ($\Delta H = -3.5 \pm 0.1$ and -4.5 ± 0.1, respectively) (*14*). Although the structure of guanidine tetraphenylborate allows for the formation of three bidentate H-bonds with the acetate moiety, only two binding steps have been observed in the calorimetric measurements (*14*). This has been attributed to the extremely unfavorable binding of an anionic guest (acetate) to the effectively anionic guanidinium-bis(acetate) complex that has a net charge of −1.

The plot of the dependence of $\nu_{a,COOH}$ frequency on the enthalpy of association of the carboxylate with guanidine derivatives indicates that the frequency of the $\nu_{a,COOH}$ is linearly proportional to the enthalpy of association. On the basis of these results, a 3 cm^{-1} downshift in the frequency of the $\nu_{a,COOH}$ can be correlated to 1 kcal/mol decrease in the enthalpy of association. These results clearly establish

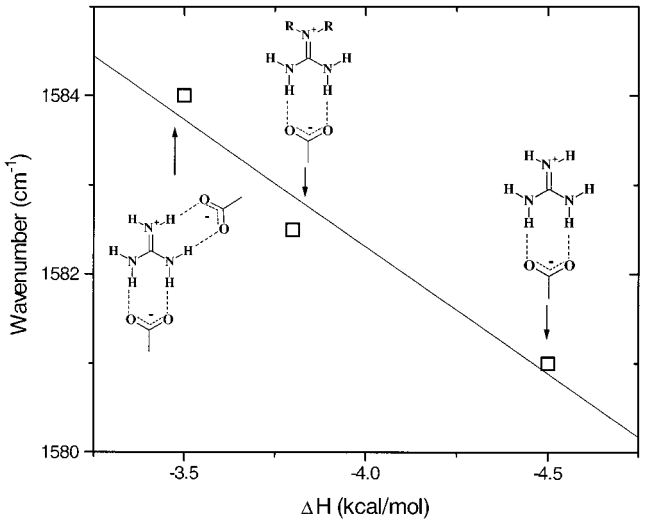

FIGURE 2: Plot of the frequency of asymmetric carboxylate vibration of ligands and the enthalpy change due to hydrogen bonding at the carboxylate moiety of tetrabutylammonium acetate to guanidinium derivatives. The enthalpy values are those obtained by Linton et al. (*14*).

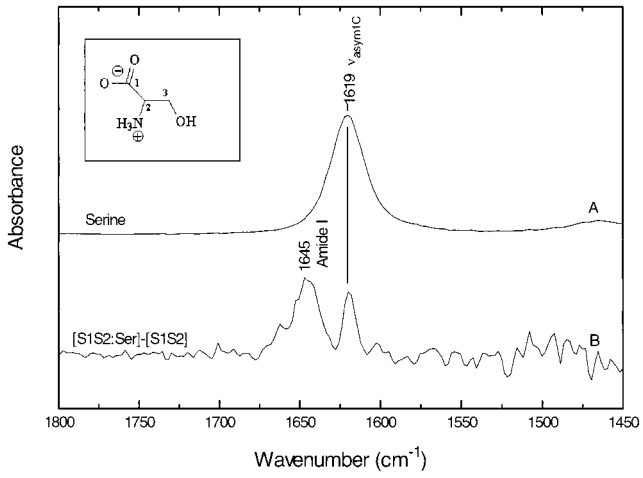

FIGURE 3: Difference FTIR spectrum between (A) serine and D_2O, (B) serine-bound and unligated form of GluR0 S1S2 protein in D_2O. The structure of serine is shown in the inset.

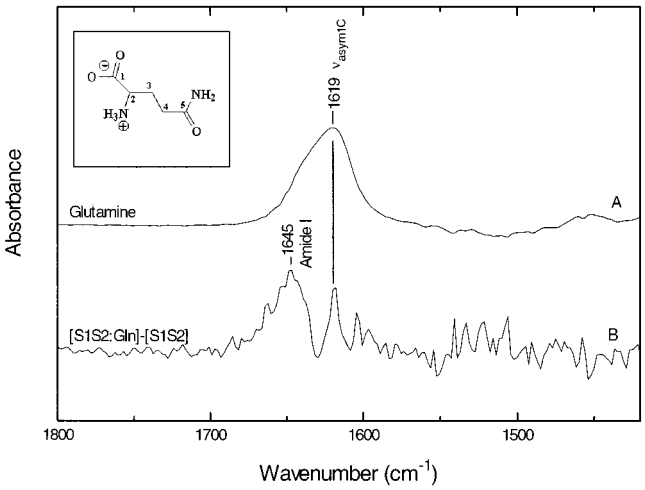

FIGURE 4: Difference FTIR spectrum between (A) glutamine and D_2O, (B) glutamine-bound and unligated form of GluR0 S1S2 protein in D_2O. The structure of glutamine is shown in the inset.

that an increase in association between the carboxylate and guanidine moieties, as evidenced by a favorable exothermic binding, results in a downshift of the absorption mode. Conversely, a negative electrostatic potential environment at the carboxylate would result in an upshift of the vibrational mode (*11*, *12*).

On the basis of the model compound studies, we conclude that the downshift of the ν_{asym1C} mode observed upon glutamate binding to the GluR0−S1S2 indicates that the noncovalent interactions, such as hydrogen bonding, and electrostatic interactions, between the 1C carboxylate of glutamate and the protein are stronger than the interactions between glutamate and D_2O. Furthermore, the model compound studies also indicate that the 2 cm^{-1} downshift can be correlated to a ~ -660 cal/mol enthalpic contribution toward the association between the 1C carboxylate of glutamate and the protein. Correspondingly, the upshift in the ν_{asym5C} mode indicates that the interactions at the 5C carboxylate of glutamate with the protein are unfavorable and could arise due to the presence of a negatively charged residue in close proximity to the negatively charged 5C carboxylate moiety.

These observations are consistent with the recent crystal structure of glutamate bound forms of the GluR0−S1S2 protein in complex with glutamate (*9*), which indicates that the 1C carboxylate of glutamate is hydrogen bonded to an arginine residue (*9*). The ionic and hydrogen bonding interactions between the positively charged arginine and negatively charged carboxylate is expected to be stronger than the interactions between the carboxylate groups and D_2O, thus accounting for the downshift in the ν_{asym1C} mode. Additionally, the crystal structure indicates the presence of the negatively charged carboxylate group of Asp 314 in close proximity to the 5C carboxylate of glutamate, which could account for the observed upshift in the ν_{asym5C} mode.

By comparing the shift in the ν_{asym1C} in D_2O with respect to that in the protein, we have examined the environment of the 1C carboxylate in serine and glutamine, which are also agonists of the prokaryotic glutamate receptor (*7*). The infrared spectra of serine in D_2O (trace A) and the difference infrared spectrum between serine bound and unligated form of GluR0−S1S2 (trace B) is shown in Figure 3. First, in the 1450 to 1800 cm^{-1} region, the vibrational spectrum of serine in D_2O exhibits a single band at 1619 cm^{-1} and on the basis of the frequency of the band and by comparison to vibrational modes of model compounds, we assign it to the ν_{asym1C} mode of serine. Second, in the difference spectrum between serine bound and unligated form of GluR0−S1S2, two absorption bands are observed in the 1450 to 1800 cm^{-1} region at 1645 and 1619 cm^{-1}. The 1645 cm^{-1} band is assigned to the amide I vibrational mode of the protein (discussed in detail in the next section), and the band at 1619 cm^{-1} is assigned to the ν_{asym1C} mode of the bound serine.

The infrared spectra of glutamine in D_2O (trace A) and the difference infrared spectrum between glutamine bound and unligated form of GluR0−S1S2 (trace B) are shown in Figure 4. These results of glutamine parallel those for serine (Figure 3), with the observation of a single band at 1619 cm^{-1} for the glutamine in D_2O, and the observation of two bands at 1645 and 1619 cm^{-1} in the difference spectrum of glutamine bound to GluR0−S1S2. The vibrational band at 1619 cm^{-1} is assigned to the ν_{asym1C} mode of glutamine, while

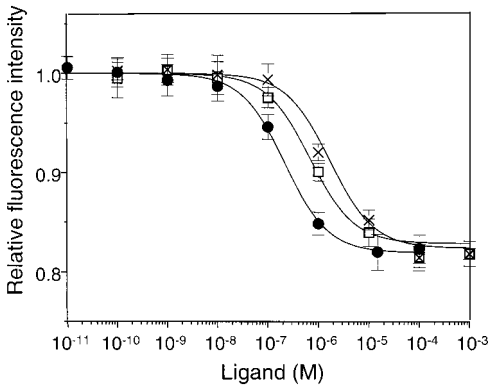

FIGURE 5: The change in the fluorescence emission intensity of 10 nM concentration of GluR0−S1S2 measured at 335 nm, as a function of glutamate (filled circles), serine (open squares), and glutamine, (crosses) concentration. Each data point represents the mean ± SEM obtained from at least three measurements. The solid lines represent the theoretical curves determined using eq 1.

the band at 1645 cm^{-1} is assigned to the amide I vibrational mode of the protein.

From the vibrational spectra of glutamine and serine in the bound and unbound forms (Figures 3 and 4), it is clear that the value of ν_{asym1C} mode (1619 cm^{-1}) for both serine and glutamine are unaltered upon binding to the protein. This suggests that the interactions, such as hydrogen bonding, at the 1C carboxylate for these two ligands with the protein are not significantly different in the protein relative to that in D_2O. The spectra, however, indicate that the width of the ν_{asym1C} mode of ligands, serine and glutamine, are significantly smaller in the protein relative to those in D_2O. The decrease in the bandwidth suggests that the dynamics of the 1C carboxylate of serine and glutamine are dampened in the protein in comparison to those in D_2O.

Secondary Structural Changes. On the basis of the difference spectra between the ligated and unligated forms of the proteins for all three ligands examined here, namely, glutamate, serine, and glutamine (Figures 1, 3, and 4), a positive feature at 1645 cm^{-1} is observed and has been assigned to the amide I vibration of the protein. The positive difference feature at 1645 cm^{-1} indicates a change in the secondary structure of the protein upon binding ligand. The exact nature of the secondary structural change cannot be clearly determined since the 1645 cm^{-1} frequency amide I vibration has been previously assigned to random structure (*15*), irregular β-sheet (*16*), and solvent exposed helices (*17*). The intensity of the positive feature at 1645 cm^{-1} relative to the ν_{asym1C} mode of the ligand is approximately the same for all three ligands (glutamate, serine, and glutamine), suggesting that the change in the secondary structure of the protein is most likely the same upon binding the three ligands.

Fluorescence Signals. The intrinsic fluorescence of GluR0−S1S2 in the unligated and ligated states of the GluR0−S1S2 protein were measured, and reported in Figure 5, using 280 nm excitation with the fluorescence monitored at the emission maximum (335 nm). At the excitation wavelength of 280 nm, the fluorescence and quantum yield of the tryptophan (Trp) residues far exceed those of other residues such as phenylalanine and tyrosine, resulting in the Trp residues to be the primary internal fluorophores. The GluR0−S1S2 protein has four Trp residues W73, 82, 281, and 376 [the numbering is based on the GluR0 full receptor sequence (*7*)], and the crystal structure suggests that all four of these residues are far from the ligand-binding domain and do not directly interact with the protein. Therefore, any changes in fluorescence observed upon ligand binding do not reflect local perturbations due to direct interactions of the tryptophan side chains with the ligand, but most likely arise due to the conformational change in the protein induced by ligand binding.

The fluorescence titration curves (shown in Figure 5) indicate that the maximum fluorescence change for the protein at saturating concentrations of the ligand is the same for the three ligands glutamate, serine, and glutamine, thus suggesting that the protein undergoes similar conformational changes upon binding these three ligands. This result is consistent with the vibrational spectra, which indicate that all three ligands induce an increase in the α-helical content of the protein, in turn yielding the positive difference feature of roughly similar intensity feature at 1645 cm^{-1} in Figures 1, 3, and 4.

The fluorescence titration curves also allow the determination of the dissociation constants for the three ligands. The K_d values for glutamate, glutamine, and serine, determined using eq 1, are 0.21 ± 0.02, 0.8 ± 0.1, 1.7 ± 0.7 μM, respectively. The K_d value for glutamate is similar to the 0.215 μM value determined by the ^{14}C-glutamate filter binding experiments (*7*). However, the K_d values for glutamine and serine are lower than the reported IC_{50} values of 16 and 30 μM respectively, obtained by competitive binding with isotopic glutamate (*7*). It is important to note that the filter binding studies were performed using a construct of GluR0−S1S2 with a longer linker relative to the construct used in the present measurements. While this difference in the constructs might account for the differences in the specific affinities of the glutamine and serine determined by filter binding studies relative to fluorescence measurements, it is unclear as to why the glutamate value appears to be consistent. Nevertheless, the trends in the affinity for the three ligands are the same for the two constructs of GluR0−S1S2, and similar to the trends in the affinities of these ligands for the full-length protein (*7*).

DISCUSSION

Ligand Affinity. The GluR0 S1S2 protein shares significant sequence similarities with the eukaryotic GluR4 S1S2 protein. Specifically, a number of the amino acid residues of GluR4−S1S2 interacting with the 1C carboxylate and amine groups of the ligand are conserved in the GluR0−S1S2 (*18*). On the basis of the vibrational spectra presented above and from previous studies of Jayaraman et al. on GluR4−S1S2 protein (*10*), the changes in the ν_{asym1C} and ν_{asym5C} modes upon glutamate binding are quite similar and consistent with the conservation of most of the amino acid residues in the GluR0−S1S2 construct. The frequency of the ν_{asym1C} mode of the bound glutamate is upshifted, and the frequency of the ν_{asym5C} mode of the bound glutamate is downshifted relative to the frequencies of these modes in D_2O in both GluR0−S1S2 and GluR4−S1S2 (*10*). However, for the glutamate bound GluR4−S1S2, we observe that $\Delta_{\nu asym1C} = -4$ cm^{-1} and $\Delta_{\nu asym5C} = +10$ cm^{-1}, while for the glutamate bound GluR0−S1S2 we observe that $\Delta_{\nu asym1C} = -2$ cm^{-1} and $\Delta_{\nu asym5C} = +3$ cm^{-1}.

As noted previously, the frequency of the asymmetric carboxylate vibration is sensitive to the extent of association between the carboxylate and guanidine moieties, and thus is an excellent probe of the strength of the ligand−protein interactions. Therefore, changes at the ν_{asym1C} mode and ν_{asym5C} mode should provide insights into the trends expected for the ligand affinity. The sum of the changes at the ν_{asym1C} mode and ν_{asym5C} mode is greater in the GluR4−S1S2 ($\Delta_{\nu asym1C} = -4$ cm^{-1} and $\Delta_{\nu asym5C} = +10$ cm^{-1}; net change $= +6$ cm^{-1}) relative to the GluR0−S1S2 ($\Delta_{\nu asym1C} = -2$ cm^{-1} and $\Delta_{\nu asym5C} = +3$ cm^{-1}; net change $= +1$ cm^{-1}). Since the net change in carboxylate frequencies is larger for GluR4−S1S2, it can be concluded that the sum of the noncovalent interactions at the two carboxylates are weaker for glutamate interacting with GluR4−S1S2 in comparison to the glutamate interacting with GluR0−S1S2. Therefore, we would expect glutamate to exhibit a lower affinity for the GluR4−S1S2 relative to the affinity for GluR0−S1S2. This is consistent with the 0.55 and 0.21 μM values for the dissociation constant of glutamate from the GluR4−S1S2 and GluR0−S1S2, respectively.

A comparison of the changes in the ν_{asym1C} mode upon binding of the ligand with the protein allows for an understanding of the differences in the interactions of the ligands with the protein. As observed previously $\Delta_{\nu asym1C} = -4$ cm^{-1} for glutamate binding to GluR0−S1S2 and $\Delta_{\nu asym1C} \sim 0$ cm^{-1} for glutamine and serine binding. These values indicate that the 1C carboxylates of serine and glutamine have relatively weaker interactions with the protein as compared to the interactions of the 1C carboxylate of glutamate with the protein. This result appears to correlate well with the lower K_d value for glutamate, relative to those for glutamine, and serine. Hence, the difference in the affinities can be partly attributed to the differences in the interactions at the 1C carboxylates.

Protein Structural Changes. The ligand binding domain of the glutamate receptors share a significant sequence and structural homology with periplasmic binding proteins (*19*). Crystal structures of a number of these proteins indicate large conformational changes in the protein induced by ligand binding. Consistent with this observation, the crystallographic structures of the apo and glutamate bound forms of the GluR2−S1S2 indicate that glutamate binding induces a large cleft closure in the bilobate structure in the GluR2−S1S2 (*8*, *9*). This structural change is consistent with the larger secondary structural changes observed in the vibrational spectra of GluR4−S1S2 upon binding glutamate (*10*). Specifically, glutamate binding to the GluR4−S1S2 leads to a significant increase in the β sheet content as well as moderate increases in the α helical and turn contents (*10*). The reported crystal structure of the GluR0−S1S2 apo form, on the other hand, exists in a closed state with no significant changes between the structures of the apo and ligated forms of the protein (*9*). Similar closed structures have been observed for the apo form of a homologous protein glucose/galatose receptor with no significant differences between the apo and ligated forms of the protein (*20*). However, in solution this protein clearly exhibited large interdomain hinge closure upon ligand binding (*21*). Comparing the results for the GluR0−S1S2 with the glucose/galatose receptor, Mayer et al. (*9*) have suggested that it is most likely that in solution the open cleft and closed cleft forms of the GluR0−S1S2 exist in rapid equilibrium, with the open cleft form being the most abundant, and the reported closed crystal structure of the apo form most likely represented an infrequently observed structure. In the present report, although the secondary structural changes induced by ligand binding are smaller in GluR0−S1S2 relative to that observed for GluR4−S1S2, both the vibrational spectra and the fluorescence measurements clearly indicate conformational changes in the protein GluR0−S1S2 induced upon ligand binding. Hence, the present results are in agreement with the hypothesis of Mayer et al. (*9*), indicating that in solution GluR0−S1S2 most likely undergoes some conformational changes upon binding the ligands glutamate, glutamine or serine.

The changes in the vibrational and fluorescence spectra, in addition, clearly indicate that serine and glutamate induce similar changes in the GluR0−S1S2 structure. This is consistent with the similar crystal structures of glutamate and serine bound forms of GluR0−S1S2 (*9*). In addition, since the glutamine bound spectrum is similar to that of glutamate and serine, it can be concluded that the glutamine bound form of GluR0−S1S2 most likely exists in the same structure as the recently determined crystal structure of glutamate and serine bound forms of GluR0−S1S2.

Comparison with the FTIR Spectra of nAChR. The ligand induced difference FTIR spectra of GluR0−S1S2 can also be compared to the extensively investigated difference spectra of the nicotinic acetylcholine receptor (nAChR) from *Torpedo* (*22*−*25*). The agonist induced difference features in the FTIR spectrum of nAChR are far more complex than those observed in the present spectra for GluR0−S1S2. Further, the bands due to the bound ligand in the nAChR spectrum are significantly smaller than the features arising due to changes in the protein. These results suggest larger structural changes induced by ligand binding in the nAChR relative to the changes in the GluR0−S1S2.

On the basis of $^2H_2O/^1H_2O$ exchange experiments, the protein difference features in the nAChR have been attributed to structural changes in the solvent-accessible extra membranous structures as opposed to changes in the hydrophobic parts of the protein present in the lipid bilayer (*24*). These changes in the solvent-accessible extra membranous structures would reflect tertiary changes in the ligand binding domain as well as the quaternary changes involving the intersubunit interface. These changes at the subunit interface are thought to play a critical role in receptor desensitization (*8*). The GluR0−S1S2, on the other hand, is expected to exhibit predominantly tertiary changes in ligand binding domain, since it exists as a dimer as opposed to the tetrameric form predicted for the full receptor (*8*, *9*). The above-mentioned differences could account for the more complex difference features of nAChR in comparison to the single band at 1645 cm^{-1} in the difference spectrum of GluR0−S1S2. However, it is also possible that the differences in magnitude of changes in nAChR vs GluR0−S1S2 to some extent reflect smaller ligand induced structural changes in the full GluR0 receptor relative to the changes in nAChR. Such a difference could account for the lower energetics associated with channel opening in the GluR0 receptor, as evidenced by the large number of spontaneous openings observed in this receptor. However, to test this hypothesis conclusively, it is necessary to compare the difference spectrum of the GluR0 in the full receptor form with the

difference spectrum of nAChR, and this will be addressed in future investigations.

ACKNOWLEDGMENT

We thank Mark Mayer for the GluR0-S1S2 construct and for optimizing the purification procedure.

REFERENCES

1. Keinanen, K., Wisden, W., Sommer, B., Werner, P., Herb, A., Verdoorn, T. A., Sakmann, B., and Seeburg, P. H. (1990) *Science 249*, 556−560.
2. Sommer, B., and Seeburg, P. H. (1992) *Trends Pharmacol. Sci. 13*, 291−296.
3. Hollmann, M., and Heinemann, S. (1994) *Annu. Rev. Neurosci. 17*, 31−108.
4. Mayer, M. L., and Westbrook, G. L. (1987) *Prog. Neurobiol. 28*, 197−276.
5. Wisden, W., and Seeburg, P. H. (1993) *Curr. Opin. Neurobiol. 3*, 291−298.
6. Hollmann, M., and Heinemann, S. (1994) *Annu. Rev. Neurosci. 17*, 31−108.
7. Chen, G.-Q., Cui, C., Mayer, M. L., and Gouaux, E. (1999) *Nature 402*, 817−821.
8. Armstrong, N., and Gouaux, E. (2000) *Neuron 28*, 165−181.
9. Mayer, M. L., Olson, R., and Gouaux, E. (2001) *J. Mol. Biol. 311*, 815−836.
10. Jayaraman, V., Keesey, R., and Madden, D. R. (2000) *Biochemistry 39*, 8693−8697.
11. Nakamoto, K. (1997) *Infrared and Raman Spectra of Inorganic and Coordination Compounds*, 5th ed., Wiley, New York.
12. Laberge, M., Sharp, K. A., and Vanderkooi, J. M. (1998) *Biophys. Chem. 71*, 9−20.
13. Spinner, E. (1967) *J. Chem. Soc. B*, 874−879.
14. Linton, B., and Hamilton, A. D. (1999) *Tetrahedron 55*, 6027−6038.
15. Byler, D. M., and Susi, H. (1986) *Biopolymers 25*, 469−487.
16. Koenig, J. L., and Tabb, D. L. (1980) in *Analytical Applications of FT-IR to Molecular and Biological Systems* (Durig, J. R., Ed.), Kluwer Academic Publishers.
17. Chapman, D., Jackson, M., and Haris, P. I. (1989) *Biochem. Soc. Trans. 17*, 617−9.
18. Chen, G. Q., Sun, Y., Jin, R., and Gouaux, E. (1998) *Protein Sci. 7*, 2623−30.
19. Quiocho, F. A., and Ledvina, P. S. (1996) *Mol. Microbiol. 20*, 17−25.
20. Flocco, M. M., and Mowbray, S. L. (1994) *J. Biol. Chem. 269*, 8931−6.
21. Careaga, C. L., Sutherland, J., Sabeti, J., and Falke, J. J. (1995) *Biochemistry 34*, 3048−55.
22. Baenziger, J. E., Miller, K. W., McCarthy, M. P., and Rothschild, K. J. (1992) *Biophys. J. 62*, 64−6.
23. Methot, N., McCarthy, M. P., and Baenziger, J. E. (1994) *Biochemistry 33*, 7709−17.
24. Baenziger, J. E., and Chew, J. P. (1997) *Biochemistry 36*, 3617−24.
25. Ryan, S. E., Blanton, M. P., and Baenziger, J. E. (2001) *J. Biol. Chem. 276*, 4796−803.

BI015729E